When Is a Molecule Properly Solvated by a Continuum Model or in a Cluster Ansatz? A First-Principles Simulation of Alanine Hydration

ARTICLE *in* THE JOURNAL OF PHYSICAL CHEMISTRY B · MARCH 2008

Impact Factor: 3.3 · DOI: 10.1021/jp077341k · Source: PubMed

3 AUTHORS:

Jens Thar
University of Leipzig
20 PUBLICATIONS **792** CITATIONS
SEE PROFILE

Stefan Zahn
University of Leipzig
38 PUBLICATIONS **1,034** CITATIONS
SEE PROFILE

Barbara Kirchner
University of Bonn
202 PUBLICATIONS **4,525** CITATIONS
SEE PROFILE

When Is a Molecule Properly Solvated by a Continuum Model or in a Cluster Ansatz? A First-Principles Simulation of Alanine Hydration

Jens Thar, Stefan Zahn, and Barbara Kirchner*

Lehrstuhl für Theoretische Chemie, Wilhelm-Ostwald-Institut für Physikalische und Theoretische Chemie, Universität Leipzig, Linnéstr. 2, D-04103 Leipzig, Germany

Received: September 12, 2007; In Final Form: November 2, 2007

In order to test the validity of the cluster ansatz approach as well as of the continuum model approach and to learn about the solvation shell, we carried out first-principles molecular dynamics simulations of the alanine hydration. Our calculations contained one alanine molecule dissolved in 60 water molecules. Dipole moments of individual molecules were derived by means of maximally localized Wannier functions. We observed an average dipole moment of about 16.0 D for alanine and of about 3.3 D for water. In particular, the average water dipole moment in proximity of alanine's COO^- group decayed continously with increasing distance, while, surprisingly, close to the CH_3 and NH_3^+ group, the dipole moment first rose before its value dropped. In a cluster ansatz approach, we considered snapshots of alanine surrounded by different water molecule shells. The dipole moments from the cluster approaches utilizing both maximally localized Wannier functions as well as natural population analysis served to approximate the dipole moments of the total trajectory. Sufficient convergence of the cluster ansatz approach is found for either of the two solvent shells around the polar groups and one solvent shell around the apolar groups or two solvent shells around the polar groups surrounded by a dieletric continuum.

1. Introduction

Water is unique in biological systems. Amino acids drastically change their chemical reactivity when dissolved in water. The most obvious effect of solvation in water is a configurational change of the amino acid from the neutral to the zwitterionic form which is reflected in a large change of the dipole moment. Thus, solvation behavior in water is one of the key questions to be addressed in biology.

The structure of the solvation shell at the example of various amino acids has been investigated by NMR spectroscopy,[1] Raman spectroscopy,[2−4] and neutron diffraction experiments.[5−9] Raman spectroscopy results suggest a solvation shell independent of the aliphatic side chain length, and neutron diffraction measurements point to differences between the solvation shell around the polar and the apolar groups. Besides these contradictory results, one should note that for the water shell only the hydrogen atoms are visible to neutron diffraction, and therefore, the positions of the oxygen atoms are derived indirectly.[10,11] There is of course a correlation between the dipole moments and experimental quantities, as for example spectroscopic and dielectric quantities.

These experimental uncertainties give rise to a wealth of computational studies of amino acids and their solvation shells. The methods employed range from classical force fields, static *ab initio* calculations, and *first-principles* molecular dynamics simulations to hybrid QM/MM methods.[12] Molecular dynamics (MD) simulations employing classical force fields are often applied to derive the structure of both solute and solvent.[13−21] Studies of dielectric properties[22] and thermodynamic data[23] were carried out. Due to their computational efficiencies, these methods are able to simulate systems of several thousand atoms in the nanosecond regime. However, the basic approach relies on empirical parameters for the description of the structure, and electrostatic interactions are restricted to fixed point charges on atoms and therefore polarization is not well described. For bulk systems, it is possible to treat polarization by empirically enlarging the permanent dipole of each molecule. Such a procedure might fail to describe the electrostatic properties sufficiently at border areas, especially in the vicinity of charged groups. Several techniques exist to add polarizability to the force field.[24,25] These rely on experimental or *first-principles* data. *Ab initio* calculations can provide vibrational spectra, structures, and electronic properties, but these methods neglect the flexible (i.e., dynamic) behavior of the amino acids or proteins and treat them as isolated molecules[18,26−38] or dissolved by a few (static) water molecules or a polarizable continuum model.[19,39−50] This can be attributed to the prohibitively high demand on computational resources when looking for a post Hartree−Fock description of the solute and a physically sound number of solvent molecules.[51] *First-principles* molecular dynamics (FPMD) simulations can be used to derive both the geometric and electronic structure.[52−60] Due to their computational demands, these methods are limited to a few hundred atoms and time scales in the picosecond regime. However, they replace the most critical drawback of standard *ab initio* methods, not to sample more than one local minima, by an efficient and temperature-dependent sampling technique. As shown by Silvestrelli and Parrinello,[61] the time scale is sufficient to converge the structure of water, and electronic properties like the dipole moment can be obtained. Recently, Degtyarenko et al.[62] carried out first-principles molecular dynamics simulation of alanine in order to discuss the solvent shell structure. Hybrid QM/MM methods[63−65] were employed to derive the structure and electronic properties of small peptides.[66−70] Huggosson et al.[71] compared the above-mentioned computational approaches to the

* Corresponding author. E-mail: bkirchner@uni-leipzig.de.

10.1021/jp077341k CCC: $40.75
Published on Web 01/15/2008

solvation pattern of dipetides. The authors found for charged groups that this pattern depends on the method employed.

For deriving electronic properties (that are not implemented in FPMD programs for technical or time-consuming reasons), there exists already for a long time[72,73] an alternative including solvation of molecules, i.e., the so-called cluster ansatz of Huber and Hermansson.[72,73] Here, a trajectory either obtained by classical or *first-principles* molecular dynamics simulations samples the configurations in the solvent. Subsequently, several of these configurations are harvested for small clusters. For molecules dissolved in liquids, these clusters normally contain the solute and its neighboring solvent molecules. Next, properties of these snapshots are evaluated using static *ab initio* calculations. The main concern with this approach is the quality of the snapshots provided by the simulation,[74] the number of snapshots, and the number of solvent molecules needed to achieve convergence with respect to the experiment.[73] Originally, this ansatz was mainly applied to obtain IR and Raman spectra of solutes[72,74,75] or to study NMR properties.[73,76,77] It was independently developed in the late 1980s by the Huber group and by the Hermansson group.[72,73]

Here, we investigate alanine as the smallest biologically active α-amino acid. The zwitterionic form of the alanine shows three sites with distinct polarity: The basic COO^- group, the acidic NH_3^+ group, and the aliphatic CH_3 group.

This article is structured as follows: First, we introduce the methods we use. This is followed by the results we obtain and their interpretation. Complementary to the work of Degtyarenko et al.,[62] we investigate the development of the structure and the dipole moment of a zwitterionic alanine in water as well as of different water shells. These local dipole moments are estimated by *first-principles* simulation in combination with maximally localized Wannier centers (MLWCs). [56,61,78−81] Furthermore, local dipole moments were experimentally investigated by Shikata.[37] Therefore, this investigation might apply also to experimental quantities, especially the test to what extent the cluster method not relying on periodic boundary conditions and with less solvent molecules produces comparable results to the full trajectory. Therefore, we cut out snapshots with different numbers of solvent molecules along the simulated trajectory and calculate local dipole moments by means of MLWCs as well as Weinhold's natural population analysis (NPA) analysis,[82] because this analysis has been proven to provide quite reliable (i.e., relative basis set independent[83]) charges. Also, we employ a conductor-like screening model[84] to test whether this approach allows one to reduce the number of solvent molecules while keeping the obtained dipole moments constant. We close this paper with a short summary of our results.

2. Technical Section

2.1. Car−Parrinello Molecular Dynamics Simulations. We simulated one alanine dissolved in 60 water molecules applying periodic boundary conditions with a box length of 1241.7 pm. All molecular dynamics simulations are based on the Car−Parrinello method[85] and are performed with the CPMD code.[86] The gradient-corrected local density functional BP86[87,88] is chosen throughout, and the Kohn−Sham orbitals are expanded in a plane wave (PW) basis with a kinetic energy cutoff of 70 Ry. Employing periodic boundary conditions, the Brillouin zone sampling is restricted to the Γ point. Norm conserving pseudopotentials of the Troullier−Martins type[89] are taken with pseudization radii of 1.05, 1.23, and 1.12 au for oxygen, carbon, and nitrogen, respectively. For all angular momenta, the same radius is used. Core−valence interaction of oxygen and nitrogen is treated by *s* and *p* potentials. The pseudopotentials are applied in the Kleinman−Bylander representation[90] with the highest angular momentum as a local potential. Hydrogen atoms are represented with a local potential. All Car−Parrinello simulations are performed in an NVE ensemble.

As a starting configuration, we took a well equilibrated structure from a previous simulation.[91]

The average computer time for a Car−Parrinello molecular dynamics step on 16 CPUs of an IBM Power4+ was 7.4 s. The additional averaged time needed for calculation of the maximally localized Wannier centers (MLWCs) was 14.8 s.

For the equilibrium simulations, the system was thermostated at 320 K using Nosé−Hoover thermostats.[92−94] The equilibration period was carried out for 1.4 ps with a Nosé−Hoover thermostat coupled to each ionic degree of freedom. A relaxation period of 1.2 ps without thermostats followed. Subsequently, the system was simulated with an average temperature of 330 K for 11.5 ps. All hydrogens are deuterated, and a 6 au time step in combination with a 900 au fictitious electron mass was applied.

Local dipole moments for CPMD calculations are derived on the basis of maximally localized Wannier centers (MLWCs).[95,96] First, the MLWCs are assigned to the closest molecule. A local dipole moment $D(M)$ of a molecule M using MLWCs is calculated according to

$$D(M) = \sqrt{\sum_{i=1}^{3} d_i^2(M)} \tag{1}$$

where the index i runs over all components of the molecule's dipole vector $\mathbf{d}(M)$. One component of the local dipole vector of molecule M with N atoms and W assigned MLWCs is calculated by

$$d_i(M) = \sum_{I=1}^{W} 2r_{Ii}(M) + \sum_{J=1}^{N} q_J(M)\, r_{Ji}(M) \tag{2}$$

with the coordinate components $r_{Ii}(M)$ of the MLWCs and $r_{Ji}(M)$ of the atoms in a system where the origin is defined by the molecule's geometric center. The charge $q_J(M)$ equals the number of valence electrons of atom J belonging to molecule M.

2.2. Static Quantum Mechanics. Density functional theory (DFT) calculations with the gradient-corrected functional BP86[87,88] were performed for isolated complexes using Turbomole,[97] version 5.9.1. All calculations with the gradient-corrected density functional BP86 were carried out in combination with the RI density fitting technique.[98] For all calculations, the Gaussian type basis set (GBS) TZVP of Schäfer et al.[99] was used. Solvent effects were modeled using the conductor-like screening model (cosmo).[84] In the cosmo model, the dielectrical constant ϵ was chosen according to water to be 78.39 and all other parameters were set to default. For the radius of the atoms, the default value "bondii radius × 1.17" was used.

Atomic charges are derived using the NPA analysis introduced by Weinhold[82] as implemented in the Turbomole package, version 5.9.1. A local dipole moment $D(M)$ of a molecule M employing Weinhold's NPA analysis is calculated according to

$$D(M) = \sqrt{\sum_{i=1}^{3} d_i^2(M)} \tag{3}$$

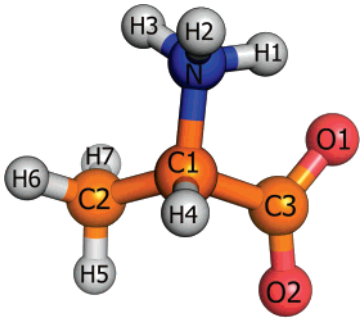

Figure 1. Geometry and labels of a single alanine molecule as used in the article.

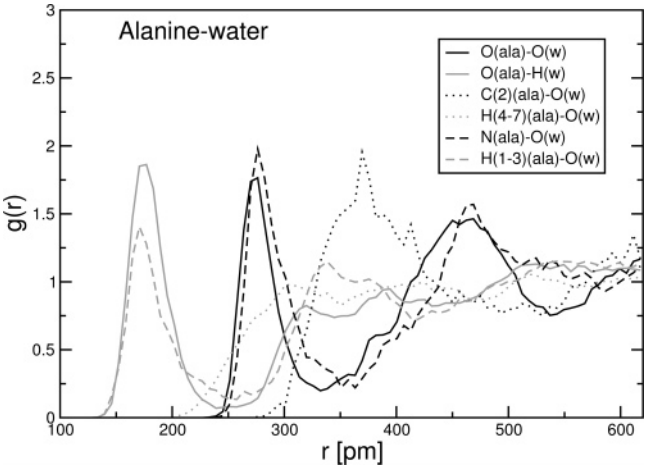

Figure 2. Radial pair distribution functions $g(r)$ with the distance r of two atoms in pm. The plot shows the distribution of distances between atoms of alanine and atoms of water.

where the index i runs over all components of the molecule's dipole vector $\mathbf{d}(M)$. One component of the local dipole vector of molecule M with N atoms is calculated by

$$d_i(M) = \sum_{I=1}^{N} q_I^{\mathrm{NPA}}(M)\, r_{Ii}(M) \qquad (4)$$

with the natural atomic charge $q_I^{\mathrm{NPA}}(M)$ of the Ith atom and its coordinate component $r_{Ii}(M)$ in a system where the origin is defined by the center of geometry of the molecule. Single point calculations as well as simulated annealing simulations with CPMD were performed with the same parameters as those presented in the previous subsection.

3. Results

3.1. Structure: Radial Pair Distribution Function. *3.1.1. Solute Functions.* In Figures 2 and 3, we show radial pair distribution functions $g(r)$ of different atoms present in our system. Figure 2 contains the functions between water and alanine atoms. We divide the hydrogen atoms of the alanine into two subgroups, the first (H(1−3)) consisting of the supposedly acidic protons of the ammonium group and the second (H(4−7)) containing the four hydrogen atoms of the aliphatic CH_n ($n = 1,3$) groups.

Alanine lacks radial symmetry and contains different "functional" groups, which on the one hand form hydrogen bonds with the hydrogen atoms of the water (COO^-) or with the oxygen atoms (NH_3^+) and on the other hand "repel" the water molecules due to their hydrophobic character (CH_3, CH). In case nothing else is stated, distances providing the g-function

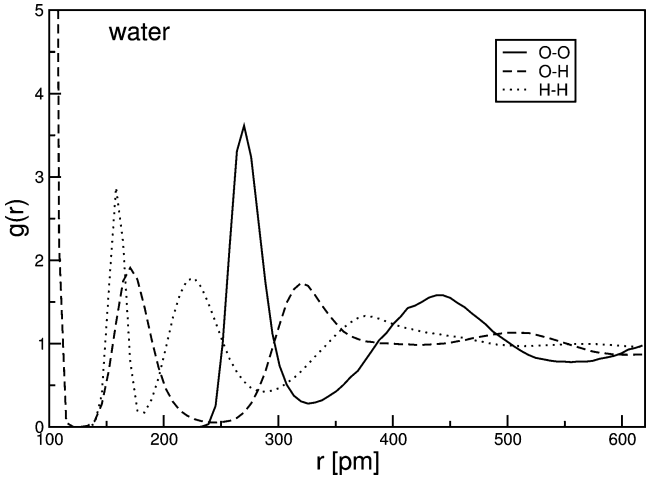

Figure 3. Radial pair distribution functions $g(r)$ with the distance r of two atoms in pm. The plot shows the distribution of distances between atoms of water molecules. w: atoms of water molecules

are measured between the discussed atom type and water's oxygen atoms. We investigate the radial pair distribution functions for each atom of the mentioned "functional" groups. Oxygen (alanine) and nitrogen display a peak around 270 pm (oxygen) and 276 pm (nitrogen), typical for a hydrogen bond donor-atom−acceptor-atom distance. Their second peak, around 460 and 475 pm, indicates the second solvation shell. As usual, this second peak is broader than the first. The g-function of the carbon atom exhibits a broad first peak around 370 pm. A second peak cannot be determined. Turning now to the hydrogen atoms of alanine, we observe a clear difference of $g(r)$ for H(1−3) as compared to H(4−7). While $g(r)$ of the former shows a peak at 171 pm, typical for rather strong hydrogen bonds, the latter exhibits a very broad local maximum close to 1 around 300 pm, indicating that the water molecules in its vicinity are virtually not structured. The second local maximum of H(1−3) is located around 355 pm and is broader than the first peak.

The radial pair distribution function of the carboxy group oxygen atoms and the water hydrogen atoms is essentially the same as the previously discussed function of H(1−3). We find a sharp maximum at 171 pm and a second, very broad one at about 355 pm. Except for the CH_3 group, no other radial distribution function decays to 1, indicating that water molecules about 600 pm away from the central atom are still structured by the alanine.

3.1.2. Solvent Functions. The functions for water are shown in Figure 3. We find the usual features of the radial distribution function, for example, an oxygen atom−oxygen atom peak around 270 pm or a hydrogen bond distance at 158 pm; see black dotted line of the O(water)−H(water) function in Figure 3. For a discussion of the radial pair distribution function of water and related problems, see ref 100, and for special discussion concerning FPMD, see ref 81. The exceptional height of the O−O function might be attributed to solute effects, in particular the enhanced polarization of the water molecules.

3.2. Dipole Moments. *3.2.1. Dipole Moments from Molecular Dynamics: Alanine.* The abbreviation PW represents CPMD calculations based on plane waves, and GBS represents calculations employing a Gaussian basis set. Figure 4 represents the distribution of the dipole moment as well as dipole moments of optimized structures for alanine dissolved in water or as an isolated molecule. *First-principles* molecular dynamics simulations have been carried out for the isolated alanine ⟨iso⟩ and the alanine dissolved in water ⟨water⟩. Static geometry optimization is performed for the isolated alanine (iso-GBS), alanine

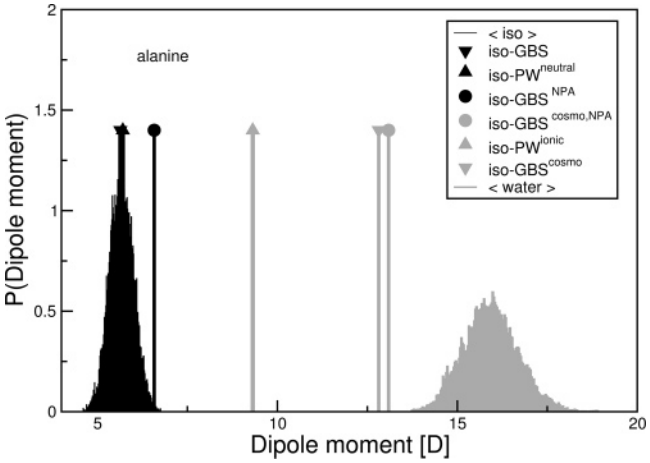

Figure 4. Probability distribution function of the dipole moment for dissolved or isolated alanine obtained from simulations or by static geometry optimization. See text for details.

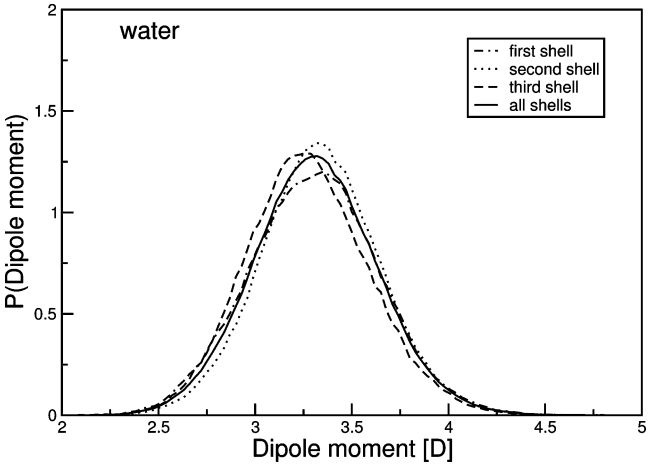

Figure 5. Probability distribution function of the dipole moment for water molecules in different shells around the alanine molecule.

"dissolved" in a set of compensation point charges (iso-GBS^{cosmo}). The label *ionic* denotes plane wave (PW) single point calculations at the geometry of the iso-GBS^{cosmo} structure, while *neutral* denotes plane wave (PW) single point calculations at the geometry of the iso-GBS structure. For geometric parameters, the reader is referred to the Supporting Information. The dipole moment provided by MLWCs (5.7 D) of one isolated alanine molecule in the neutral state (iso-PW^{neutral}) excellently matches the "integrated" dipole moment, that is, the dipole moment obtained from calculating the expectation value of the position operator, of 5.6 D for an isolated molecule optimized with the Gaussian basis set (iso-GBS). This observation encourages us to directly compare dipole moments obtained by integration with dipole moments calculated on the basis of MLWCs.

Also, the mean dipole moment value (⟨iso⟩, 5.7 D) obtained from a trajectory which started from the zwitterionic structure but rearranged to the neutral form during equilibration gives the same result as the iso-PW^{neutral} calculation. In contrast, the dipole moment based on the NPA analysis (iso-GBS^{NPA}) yields a value about 0.9 D too large (6.6 D). Not surprisingly, enforcing the zwitterionic structure (iso-PW^{ionic}) yields a significantly enlarged dipole moment of about 9.3 D. Adding a conductor-like screening model increases the dipole moment to 12.8 D (iso-GBS^{cosmo}). Here, the value provided by the NPA analysis (13.1 D) is in good agreement with its "integrated" counterpart. However, the continuum model ansatz does not represent the solvent completely, because an explicit solvation with 60 water molecules yields an average dipole moment of 15.9 D during the simulation.

3.2.2. Dipole Moment from Dynamics: Water. Figure 5 shows the probability distribution function of the dipole moment for all water molecules as well as water molecules inside certain shells around the alanine molecule. Different solvent shells were selected according to the radial distribution function presented in Figure 2. A water molecule is always assigned to the closest group determined by the distance of its oxygen atoms, so that these groups are rather the origin of a cone of water molecules than the center of a sphere. The first shell around the oxygen atom contains all water molecules up to a distance of 330 pm, the second shell contains all water molecules from 330 pm up to a distance of 540 pm, and further solvent molecules are collected in the third shell. For nitrogen, these two cutoffs are set to 360 and 590 pm. For the carbon atoms, the first shell consists of water molecules up to a distance of 510 pm, and all further solvent molecules are collected in the second shell. In accordance with Figure 2, no third shell is defined for the carbon atoms.

The average dipole moment of a water molecule is about 3.3 D, which is larger than an average dipole moment of 2.95 D found for pure water by Silvestrelli and Parrinello.[61] For water dissolving H_2[101] and DMSO,[78] dipole moments of 2.97 and 2.96 D have been reported. We want to add that the statistical error of all average values given here is well below 0.01 D. In the following, this allows us to compare relatively subtle differences in the average dipole moment of distinct water shells.

We observe an unusual behavior of the average dipole moment for different water shells around the alanine: The first shell shows an average dipole moment of 3.29 D, the second shell contains water molecules with an average dipole moment of 3.32 D, and the dipole moment drops to 3.25 D for water molecules beyond the second shell. This means that the average dipole moment of water is not maximal in the direct vicinity of alanine. In contrast, it reaches its maximum within the second shell and decreases afterward. The deviation of the three investigated shells from the total average is rather small. On the one hand, this could indicate the dipole moment being rather independent from the structure of the liquid. On the other hand, each shell includes water molecules in a vastly different electrostatic environment (NH_3^+, CH_3, COO^-) with a different influence on the dipole, and these influences might cancel each other.

However subtle these trends are, they are clearly detectable and we can further determine their origin by the following procedure: We investigate the dipole moment of water molecules around each of the three distinct functional groups NH_3^+, CH_3, and COO^-. The probability distributions of the dipole moment from different shells inside each of these cones is depicted in Figure 6.

The average dipole moment of the carboxy group decays from 3.35 D (first shell) over 3.31 D (second shell) to 3.25 D (third shell), in a usual manner as would be expected. For the CH_3 group, we find an average dipole moment of 3.27 D (first shell) rising to 3.36 D (second shell). The ammonium group shows an average dipole moment of 3.28 D for its first shell, rising to 3.30 D (second shell) and then dropping to 3.27 D for the third shell. Thus, the average dipole moment of the solvent molecules in the vicinity of the COO^- decays with rising distance from the solute. In contrast, the average dipole moment of the solvent molecules around the CH_3 and NH_3 groups of alanine rise when entering the second shell. A similar behavior was observed

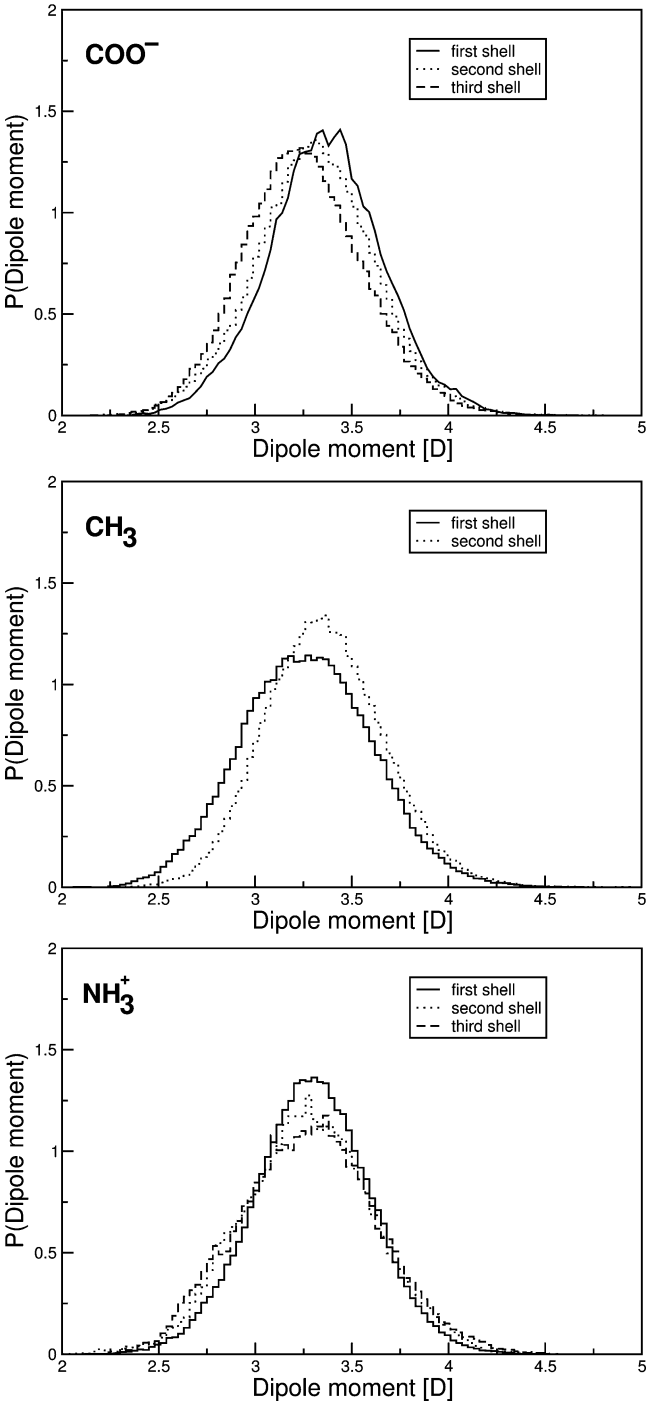

Figure 6. Probability distribution function of the dipole moments of water molecules closest to atoms of the COO^-, CH_3, and NH_3^+ groups of the alanine. See text for details.

previously for H_2 in H_2O,[101] where the dipole moment of the water molecules surrounding the H_2 molecule also showed a local maximum. The error bars are in a similar range as discussed previously by Silvestrelli and Parrinello.[61]

3.2.3. Dipole Moments from Static Calculations: Alanine. We now turn to the evaluation of the local dipole moments for snapshots without periodic boundary conditions along the trajectory according to the cluster ansatz. We selected four distinct sets of snapshots: The first two sets only account for the first (and second) solvent shell of the two polar groups. The second two sets account for the first (and second) solvent shell of all selected subgroups. We use this procedure for the following reasons:

TABLE 1: Average Total Dipole Moment in D of Two Sets for Different Numbers of Snapshots

system	10	20	30	40	50	60	80	100
set0	11.14	11.16	11.00	11.06	10.99	11.07	11.08	11.01
set1	15.85	15.60	16.14	15.82	15.78	15.84	15.84	15.79

TABLE 2: Average Total Dipole Moments in D of the Complete Systems, including Alanine and Different Embedding Shells of Water (set0−set4) (See Text for Further Details)

method	**set0**	**set1**	**set2**	**set3**	**set4**
PW/MLWC	10.99	15.78	11.76	12.77	8.09
GBS/dens	10.56	15.65	11.53	12.66	8.25
GBS/NPA	12.13	14.09	11.89	11.45	9.26
GBS^{cosmo}/dens	13.98	17.88	13.75	14.58	9.85
GBS^{cosmo}/NPA	14.39	14.93	12.60	12.03	9.76

(1) First, we want to know whether the use of periodic boundary conditions is necessary for the computation of the solute's (i.e., the alanine's) electronic properties or if these properties are sufficiently converged already with two or even less layers of solvent molecules added. In order to test this, CPMD calculations employing the Poisson solver developed by Tuckerman[102] have been carried out for the four sets of snapshots and the dipole moments have been evaluated using maximally localized Wannier centers; that is, we want to investigate for which cluster size the cluster method is valid.

(2) Second, we want to investigate whether the same convergence can be obtained by using Weinhold's NPA analysis in combination with a Gaussian basis set. This setup is computationally less demanding and also gives direct access to atomic point charges, which are discussed in the Supporting Information. One should add here that, in contrast to the Wannier center analysis, the atomic charges on each molecule do not necessarily add up to zero. Because the dipole moment of a charged system depends on its origin, we always relate the molecular dipole moment to the geometrical center of the molecule.

(3) Our third concern regards the influence of a polarizable continuum on the electronic properties. As already shown in section 3.1.2, the application of a polarizable continuum model yields at least the qualitatively right structure of the alanine. Here, we want to test if the addition of the polarizable continuum model converges the electronic properties even faster, that is, with less solvent shells.

Table 2 summarizes test calculations of the total dipole moment of the isolated zwitterionic alanine (**set0**) as well as alanine and different sets of solvent shells; see Figure 7. **Set1** consists of 50 snapshots of alanine and the first shell around the NH_3^+ and COO^- group. This set contains on average seven water molecules. Water molecules "belonging", that is, closest, to these two groups are indexed as "ionic" throughout this section. **Set2** is **set1** complemented by the second shell of the ionic groups and is constituted of about 27 water molecules. **Set3** is **set1** supplemented by the first shell of the CH_3 group. Water molecules inside the shells of subgroup 3 are indexed as "aliphatic" throughout this section. **Set3** exhibits 17 water molecules on average. **Set4** is the set union of **set2** and **set3**, with about 36 water molecules included.

Table 1 summarizes convergence tests of the total dipole moment of different systems with respect to the number of snapshots considered. We investigated three distinct systems extracted from the trajectory: The isolated alanine **set0** and **set1**. Isolated alanine serves as a direct reference for the average dipole moment in Table 2, while **set1** is used to test whether

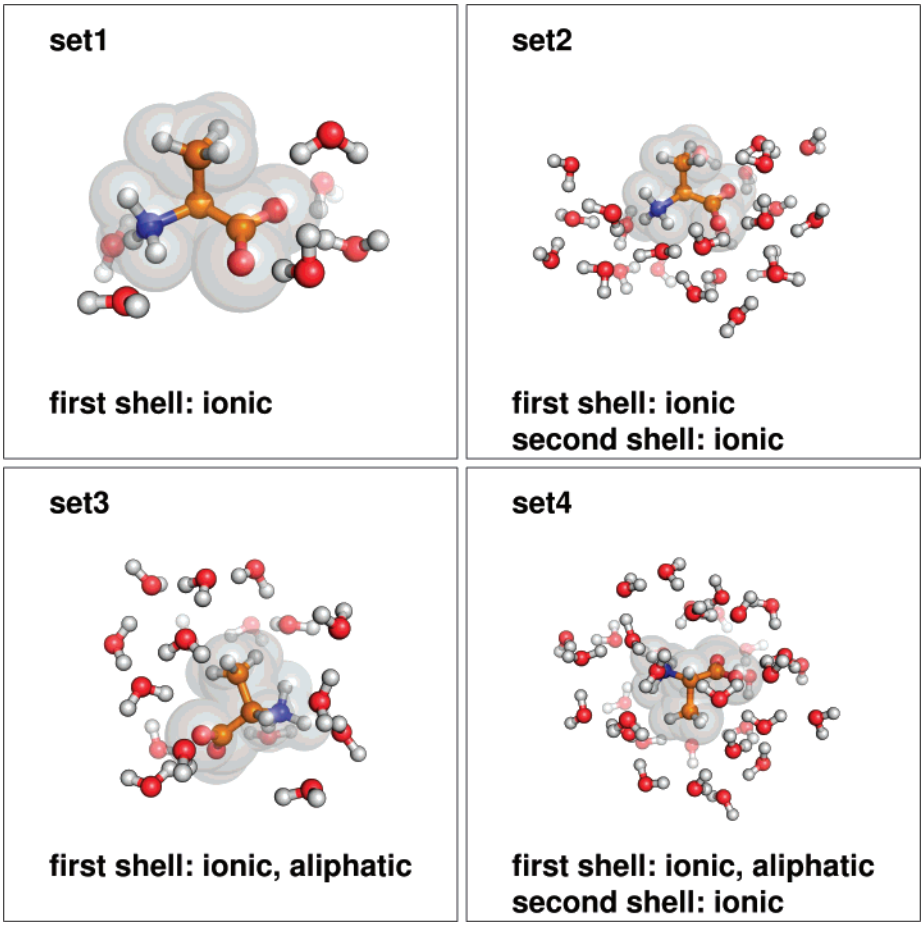

Figure 7. Snapshot with different shells of solvent molecules. See text for details.

the additional variance introduced by a different number of molecules in each snapshot results in a more unfavorable convergence behavior.

For the isolated alanine, convergence up to a difference of 0.1 D is achieved with already 30 snapshots. Due to the fluctuating number of molecules, **set1** converges slightly slower, and at least 40 snapshots are needed to obtain meaningful statistics. We want to add that this rather fast convergence can also be attributed to a short overall simulation time of about 11.5 ps, which restricts the sampled configurations of alanine to quite a small portion of phase space. To ensure a certain degree of accuracy, we always chose a set of 50 snapshots. For other properties, the convergence behavior might need more than 50 snapshots, which is why we consider this number to be the lower boundary.

The electronic charge distribution used for the calculation of the dipole moment is either given by maximally localized Wannier centers (MLWC), given by the density (dens), or incorporated into the atomic charges by means of Weinhold's natural population analysis. We find good agreement comparing the dipole moment obtained by PW/MLWC and the usual quantum mechanical treatment (GBS/dens). Therefore, we take the dipole moment of the CPMD simulation as the reference, and differences between different sets are discussed on the basis of the PW/MLWC calculations if not otherwise stated. Comparing the dipole moments obtained by means of NPA, either or not embedded in a polarizable continuum, with the corresponding quantum mechanical dipole moment (GBS/dens), we observe reasonably good agreement with a maximal deviation of about 15%. Compare the second and third and fourth and fifth rows, respectively. We also observe that the total dipole moment of the system decreases when changing from **set0** without any water molecules to **set4** with about 40 water molecules. Thus, the total dipole moment converges to the small values of arbitrarily distributed bulk water. For the same reason, the gap between dipole moments calculated with and without a polarizable continuum model becomes smaller with rising number of water molecules.

TABLE 3: Average Local Dipole Moments in D of Alanine within Snapshots including Different Shells of Solvent Molecules (See Text for Further Details)

method	**set0**	**set1**	**set2**	**set3**	**set4**	**all**
PW/MLWC	10.99	14.10	15.08	14.59	15.56	
GBS/NPA	12.13	12.86	13.14	13.15	13.45	
GBS^{cosmo}/NPA	14.39	13.67	13.45	13.62	13.51	
PW^{PBC}/MLWC						15.93

The influence of different solvent shells on the local dipole moment of alanine is summarized in Table 3. A complete neglect of the solvent reduces the dipole moment to about 62.5% of the reference value; compare the first entry in Table 3 with the PW^{PBC}/MLWC value of 15.93 D. Considering **set1**, the inclusion of first shell water molecules around the polar groups provides the largest correction of about 20% of the reference dipole moment. Obviously, the net effect of adding a second shell around the polar groups (**set2**) is larger than the inclusion of the first shell around the apolar group of alanine (**set3**). **Set4** is already a reasonably good approximation to the periodic boundary conditions, yielding about 98% of the reference dipole moment. Thus, for accurately reproducing the results of the periodic boundary calculations, we recommend using a solvent shell similar to **set4**. Except for the isolated alanine, utilizing NPA for **sets1−4** yields dipole moments which underestimate

TABLE 4: Average Dipole Moments in D of Water Molecules within Different Solvent Shells (See Text for Further Details; Please Note, in set3, There Are Only Ionic First Shell Waters, and in set1 and set2, There Are No Aliphatic Waters Included)

	H_2O^{ionic}						$H_2O^{aliphatic}$	
	first shell				second shell		first shell	
method	**set1**	**set2**	**set3**	**set4**	**set2**	**set4**	**set3**	**set4**
PW/MLWC	2.30	2.94	2.48	3.15	2.62	2.70	2.52	2.66
GBS/NPA	2.75	**2.87**	2.79	*2.90*	2.77	2.79	2.77	2.80
GBS^{cosmo}/NPA	**2.86**	*2.91*	2.88	2.92	2.85	2.86	2.86	2.87
PW^{PBC}/MLWC	3.32				3.30		3.27	

the dipole moment compared to the reference. In contrast to the PW/MLWC calculations, GBS/NPA calculations do not show much difference between **set2** and **set3**. Thus, adding the second ionic water shell seems to be equivalent to adding the first apolar shell in this case. For GBS^{cosmo}/NPA, the alanine dipole moment is largest if the conductor-like screening model is as close as possible to the polar groups; see **set0**, **set1**, and **set3**. Furthermore, comparing the dipole moment of **set4** for GBS/NPA and GBS^{cosmo}/NPA, the difference of only 0.07 D indicates that the contribution of the polarizable continuum is almost zero. This supports our previous conclusion that **set4** is already a good approximation to trajectories obtained with periodic boundary conditions when aiming at properties related to the electronic dipole moment and it is not necessary to apply an additional conductor-like screening model. On the other hand, using cosmo in addition to only one shell of solvent molecules provides almost the same results as **set4** in a more efficient manner. When we add more and more solvent molecules, we also see that the average dipole moment of alanine dissolved in a conductor-like screening model decays in contrast to both PW/MLWC and GBS/NPA. This means that cosmo tends to overpolarize the molecules solved in it.

3.2.4. Dipole Moments from Static Calculations: Water. Table 4 shows the average dipole moments of water molecules surrounding alanine. Water molecules of **set1** exhibit a dipole moment of about 70% of the reference dipole moment of 3.32 D; see the last line of Table 4. Obviously, adding water molecules at the apolar site of alanine (**set3**) induces only a small correction of about 0.18 D to the dipole moment of the first shell. In contrast, adding a second layer of water molecules between the water molecules covering the ionic site of alanine and the vacuum provides a correction of about 0.64 D, providing nearly 90% of the reference dipole moment. This is obvious, because in this set the water molecules are better solvated, whereas in **set1** they are not solvated at the interface to the vacuum.

In agreement with the conclusions drawn from Table 3, **set4** is also a good approximation for the dipole moment of the water molecules in the first solvation shell, although these water molecules are "solvated" by only one water shell. It is reflected by the dipole moment of 3.15 D representing only 95% of the reference value. The dipole moment of the second shell's water molecules is 0.32 or 0.22 D larger compared to the dipole moments of the first shell's water molecules of **set1** and **set3**. This can be explained by the portion of the surface exposed to the vacuum. The larger this surface (as for **set1**), the smaller the dipole moment.

For the same reason, the dipole moment of water molecules around the apolar group of alanine (**set3**) is 0.22 D larger than the dipole moments of their ionic counterparts; they are therefore more comparable to the second shell's water molecules of **set2** and **set4**. GBS/NPA yields essentially the same trends as PW/MLWC, but differences between different sets are much smaller. This is emphasized by a maximal spread of 0.15 D ($|\mu|^{\mathbf{set4}} - |\mu|^{\mathbf{set1}}$) compared to a spread of 0.85 D observed for PW/MLWC. Regarding $|\mu|^{\mathbf{set1}}$ (GBS^{cosmo}/NPA) and $|\mu|^{\mathbf{set2}}$ (GBS/NPA) as well as $|\mu|^{\mathbf{set3}}$ (GBS^{cosmo}/NPA) and $|\mu|^{\mathbf{set4}}$ (GBS/NPA), we can conclude again that the addition of the polarizable continuum model is essentially equivalent to the introduction of one water shell.

4. Conclusion

We studied the structure and electronic properties of alanine dissolved in water with *first-principles* molecular dynamics as well as with the cluster method of Huber and Hermansson.[72,73] The cluster method can be shortly described as the calculation of smaller or equally large snapshots cut out along a trajectory. The reliability of the cluster method was gauged against the results of *first-principles* molecular dynamics simulation.

The structure of the water molecules surrounding the alanine is largely determined by the subgroups of the alanine. While the charged NH_3^+ and COO^- groups form hydrogen bond networks with their nearest neighboring water molecules, the aliphatic CH_3 group lacks this network and, as a consequence, exhibits a broader first water shell. Zwitterionic alanine dissolved in 60 explicit water molecules shows a dipole moment of 16 D being about 45% larger than if isolated. The same zwitterionic alanine molecules surrounded by the conductor-like screening model exhibit a dipole moment of 13 D, indicating that this model alone is not sufficient to provide quantitatively correct results for electronic properties of dissolved molecules like alanine. This is an important result regarding the fact that many studies on electronic properties of hydrated molecules rely on such continuum models only. The large increase of the dipole moment in water must have several implications for the alanine properties such as change of functionality.

For the water molecules, we found an average dipole moment of 3.3 D, an about 10% larger value than previously found for bulk water. This might be attributed to inducing forces of the alanine molecule. There are distinct differences between the average dipole moment of water molecules depending on their position relative to the functional groups of the solute. Surprisingly, water molecules in the second water shell around the CH_3 group exhibit the largest average dipole moment of 3.36 D of all water shells. The dipole moment in shells around the COO^- behaves according to intuition: The innermost shell features the largest average dipole moment, which decays with rising distance. Surprisingly, the NH_3^+ group behaves in contrast to its anionic counterpart. This functional group possesses a slight maximum of the dipole moment in its second water shell. It remains open whether this is a feature of a water shell formed by an ammonium group or whether these water molecules are structured by the shells around the COO^- and CH_3 group as a secondary effect. This effect was determined previously for an investigation of the hydrophobic hydration from FPMD.[101]

The cluster ansatz as well as its reference was partially treated on the same footing, that is, the same theoretical level. Therefore, deviations are only caused by the absence of water molecules in the cluster ansatz, and we were able to estimate how many water molecules have to be included in a cluster calculation to converge the average dipole moment of alanine. We found that two shells of water molecules around the ionic groups and one shell around the aliphatic group are enough to reasonably converge the dipole moment of the alanine to about 98% of the full simulation. Due to the very broad first solvation shell of CH_3, all atoms of the alanine are surrounded by an equally thick

water shell. The achieved level of convergence indicates that a simulation box with 60 water molecules is already adequately large to converge properties of the solute. For the number of snapshots, we found that at least 50 snapshots are needed to reproduce a 10 ps trajectory. This might be too scarce for other properties of the solute and should be considered as a lower boundary.

Dipole moments provided by Weinhold's NPA analysis are less dependent on the number of surrounding molecules. Therefore, the dipole moment is overestimated for isolated alanine and underestimated for dissolved alanine. However, the dipole moments obtained are still as large as 84−89% of the reference value and show the correct trend when further adding solvent molecules.

It is important to note that the conductor-like screening model on its own does not reproduce the solvent effects quantitatively correctly. This continuum approximation shows similar effects as one additional solvent shell. As stated above, at least two shells are needed to converge the dipole moment of the solute sufficiently. Thus, it is recommended to add at least one explicit solvent shell if computationally feasible, when applying the conductor-like screening model approximation.

Acknowledgment. This work was supported with computational time provided by the NIC supercomputers in Jülich. We also would like to thank Prof. Neese (Bonn) for allowing us to use the local cluster. The authors gratefully acknowledge the financial support of the DFG priority program SPP 1191 "Ionic Liquids" and the ERA Chemistry program, that allows fruitful collaboration under the project "A Modular Approach to Multi-responsive Surfactant/Peptide (SP) and Surfactant/Peptide/Nanoparticle (SPN) Hybrid Materials". We furthermore would like to thank the collaborative research center SFB 624 "Templates" at the University of Bonn for financial support. J.T. acknowledges funding by a "Chemiefonds-Stipendium" of the Fonds der Chemischen Industrie.

Supporting Information Available: Discussion, figures, and tables on static quantum mechanics, geometrical parameters of alanine, and atomic point charges. This material is available free of charge via the Internet at http://pubs.acs.org.

References and Notes

(1) Spisni, A.; Gotsis, E. D.; Fiat, D. *Biochem. Biophys. Res. Commun.* **1986**, *135*, 363−366.
(2) Fischer, W. B.; Eysel, H. H. *J. Mol. Struct.* **1997**, *415*, 249−257.
(3) Hecht, D.; Tadesse, L.; Walters, L. *J. Am. Chem. Soc.* **1993**, *115*, 3336−3337.
(4) Ide, M.; Maeda, Y.; Kitano, H. *J. Phys. Chem. B* **1997**, *101*, 7022−7026.
(5) Kameda, Y.; Ebata, H.; Usuki, T.; Uemura, O.; Misawa, M. *Bull. Chem. Soc. Jpn.* **1994**, *67*, 3159−3164.
(6) Kameda, Y.; Sugawara, K.; Usuki, T.; Uemura, O. *Bull. Chem. Soc. Jpn.* **2003**, *76*, 935−943.
(7) Kameda, Y.; Sasaki, M.; Yaegashi, M.; Tsuji, K.; Oomori, S.; Hino, S.; Usuki, T. *J. Solution Chem.* **2004**, *33*, 733−745.
(8) McLain, S. E.; Soper, A. K.; Terry, A. E.; Watts, A. *J. Phys. Chem. B* **2007**, *111*, 4568−4580.
(9) McLain, S. E.; Soper, A. K.; Watts, A. *J. Phys. Chem. B* **2006**, *110*, 21251−21258.
(10) Soper, A. K.; Bruni, F.; Ricci, M. A. *J. Chem. Phys.* **1997**, *106*, 247−254.
(11) Soper, A. K.; Phillips, M. G. *Chem. Phys.* **1986**, *107*, 47−60.
(12) Kirchner, B.; Wennmohs, F.; Ye, S. F.; Neese, F. *Curr. Opin. Chem. Biol.* **2007**, *11*, 134−141.
(13) Karplus, M.; Mccammon, J. A. *Nature* **1979**, *277*, 578−578.
(14) Duan, Y.; Kollman, P. A. *Science* **1998**, *282*, 740−744.
(15) Elstner, M.; Frauenheim, T.; Kaxiras, E.; Seifert, G.; Suhai, S. *Phys. Status Solidi B* **2000**, *217*, 357−376.
(16) Gnanakaran, S.; Garcia, A. *J. Phys. Chem. B* **2003**, *107*, 12555−12557.
(17) Madan, B.; Sharp, K. *Biophys. Chem.* **1999**, *78*, 33−41.
(18) Mu, Y.; Kosov, D.; Stock, G. *J. Phys. Chem. B* **2003**, *107*, 5064−5073.
(19) Ono, S.; Kuroda, M.; Higo, J.; Nakajima, N.; Nakamura, H. *J. Comput. Chem.* **2002**, *23*, 470−476.
(20) Sagarik, K.; Dokmaisrijan, S. *THEOCHEM* **2005**, *718*, 31−47.
(21) Tobias, D. J.; Brooks, C. L. *J. Phys. Chem.* **1992**, *96*, 3864−3870.
(22) Boresch, S.; Willensdorfer, M.; Steinhauser, O. *J. Chem. Phys.* **2004**, *120*, 3333−3347.
(23) Hess, B.; van der Vegt, N. *J. Phys. Chem. B* **2006**, *110*, 17616−17626.
(24) van Maaren, P.; van der Spoel, D. *J. Phys. Chem. B* **2001**, *105*, 2618−2626.
(25) Yu, H. B.; van Gunsteren, W. F. *Comput. Phys. Commun.* **2005**, *172*, 69−85.
(26) Alkorta, I.; Elguero, J. *THEOCHEM* **2004**, *680*, 191−198.
(27) Brijbassi, S. U.; Sahai, M. A.; Setiadi, D. H.; Chass, G. A.; Penke, B.; Csizmadia, I. G. *THEOCHEM* **2003**, *666−667*, 291−301.
(28) Chaudhuri, P.; Canuto, S. *THEOCHEM* **2002**, *577*, 267−279.
(29) Dale Keefe, C.; Pearson, J. K. *THEOCHEM* **2004**, *679*, 65−72.
(30) Ellzy, M. W.; Jensen, J. O.; Hameka, H. F.; Kay, J. G. *Spectrochim. Acta, Part A* **2003**, *59*, 2619−2633.
(31) Hudaky, I.; Perczel, A. *THEOCHEM* **2003**, *630*, 135−140.
(32) Kapitan, J.; Baumruk, V.; Kopecky, V.; Bour, P. *J. Phys. Chem. A* **2006**, *110*, 4689−4696.
(33) Klipfel, M.; Zamora, M.; Rodriguez, A.; Fidanza, N.; Enriz, R.; Csizmadia, I. *J. Phys. Chem. A* **2003**, *107*, 5079−5091.
(34) Perczel, A.; Farkas, Ö.; Jákli, I.; Topol, I. A.; Csizmadia, I. G. *J. Comput. Chem.* **2003**, *24*, 1026−1042.
(35) Selvarengan, P.; Kolandaivel, P. *THEOCHEM* **2004**, *671*, 77−86.
(36) Selvarengan, P.; Kolandaivel, P. *J. Mol. Model.* **2004**, *10*, 198−203.
(37) Shikata, T. *J. Phys. Chem. A* **2002**, *106*, 7664−7670.
(38) Vargas, R.; Garza, J.; Hay, B.; Dixon, D. *J. Phys. Chem. A* **2002**, *106*, 3213−3218.
(39) Ahn, D.-S.; Park, S.-W.; Jeon, I.-S.; Lee, M.-K.; Kim, N.-H.; Han, Y.-H.; Lee, S. *J. Phys. Chem. B* **2003**, *107*, 14109−14118.
(40) Frimand, K.; Bohr, H.; Jalkanen, K. J.; Suhai, S. *Chem. Phys.* **2000**, *255*, 165−194.
(41) Han, W.-G.; Jalkanen, K.; Elstner, M.; Suhai, S. *J. Phys. Chem. B* **1998**, *102*, 2587−2602.
(42) Jalkanen, K. J.; Elstner, M.; Suhai, S. *THEOCHEM* **2004**, *675*, 61−77.
(43) Jalkanen, K. J.; Nieminen, R. M.; Frimand, K.; Bohr, J.; Bohr, H.; Wade, R. C.; Tajkhorshid, E.; Suhai, S. *Chem. Phys.* **2001**, *265*, 125−151.
(44) Kang, Y. K. *THEOCHEM* **2004**, *675*, 37−45.
(45) Kikuchi, O.; Watanabe, T.; Ogawa, Y.; Takase, H.; Takahashi, O. *J. Phys. Org. Chem.* **1997**, *10*, 145−151.
(46) Kohtani, M.; Breaux, G.; Jarrold, M. *J. Am. Chem. Soc.* **2004**, *126*, 1206−1213.
(47) Park, S.-W.; Ahn, D.-S.; Lee, S. *Chem. Phys. Lett.* **2003**, *371*, 74−79.
(48) Sebek, J.; Gyurcsik, B.; Sebestik, J.; Kejik, Z.; Bednarova, L.; Bour, P. *J. Phys. Chem. A* **2007**, *111*, 2750−2760.
(49) Sicinska, D.; Paneth, P.; Truhlar, D. *J. Phys. Chem. B* **2002**, *106*, 2708−2713.
(50) Tajkhorshid, E.; Jalkanen, K.; Suhai, S. *J. Phys. Chem. B* **1998**, *102*, 5899−5913.
(51) Neese, F.; Petrenko, T.; Ganyushin, D.; Olbrich, G. *Coord. Chem. Rev.* **2007**, *251*, 288−327.
(52) Leung, K.; Rempe, S. *J. Am. Chem. Soc.* **2004**, *126*, 344−351.
(53) Leung, K.; Rempe, S. B. *J. Chem. Phys.* **2005**, *122*, 184506−12.
(54) Wei, D. Q.; Guo, H.; Salahub, D. R. *Phys. Rev. E* **2001**, *6401*, 011907.
(55) Aktah, D.; Passerone, D.; Parrinello, M. *J. Phys. Chem. A* **2004**, *108*, 848−854.
(56) Boero, M.; Terakura, K.; Ikeshoji, T.; Liew, C. C.; Parrinello, M. *Phys. Rev. Lett.* **2000**, *85*, 3245−3248.
(57) Buch, V.; Mohamed, F.; Parrinello, M.; Devlin, J. P. *J. Chem. Phys.* **2007**, *126*, 074503.
(58) Devlin, J. P.; Buch, V.; Mohamed, F.; Parrinello, M. *Chem. Phys. Lett.* **2006**, *432*, 462−467.
(59) Iannuzzi, M.; Parrinello, M. *Phys. Rev. B* **2002**, *66*, 155209.
(60) Kreitmeir, M.; Bertagnolli, H.; Mortensen, J. J.; Parrinello, M. *J. Chem. Phys.* **2003**, *118*, 3639−3645.
(61) Silvestrelli, P. L.; Parrinello, M. *J. Chem. Phys.* **1999**, *111*, 3572−3580.
(62) Degtyarenko, I.; Jalkanen, K.; Gurtovenko, A.; Nieminen, R. *J. Phys. Chem. B* **2007**, *111*, 4227−4234.
(63) Laio, A.; VandeVondele, J.; Rothlisberger, U. *J. Chem. Phys.* **2002**, *116*, 6941−6947.

(64) Thar, J.; Reckien, W.; Kirchner, B. *Top. Curr. Chem.* **2007**, 133−171.
(65) Sinnecker, S.; Neese, F. *J. Comput. Chem.* **2006**, *27*, 1463−1475.
(66) Warshel, A.; Levitt, M. *J. Mol. Biol.* **1976**, *103*, 227−249.
(67) Field, M. J.; Bash, P. A.; Karplus, M. *J. Comput. Chem.* **1990**, *11*, 700−733.
(68) Nemukhin, A. V.; Grigorenko, B. L.; Bochenkova, A. V.; Kovba, V. M.; Epifanovsky, E. M. *Struct. Chem.* **2004**, *15*, 3−9.
(69) Topf, M.; Varnai, P.; Richards, W. *J. Am. Chem. Soc.* **2002**, *124*, 14780−14788.
(70) Yang, Y.; Cui, Q. *J. Phys. Chem. B* **2007**, *111*, 3999−4002.
(71) Hugosson, H. W.; Laio, A.; Maurer, P.; Rothlisberger, U. *J. Comput. Chem.* **2006**, *27*, 672−684.
(72) Hermansson, K.; Knuts, S.; Lindgren, J. *J. Chem. Phys.* **1991**, *95*, 7486−7496.
(73) Eggenberger, R.; Gerber, S.; Huber, H.; Searles, D.; Welker, M. *J. Chem. Phys.* **1992**, *97*, 5898−5904.
(74) Pejov, L.; Spangberg, D.; Hermansson, K. *J. Phys. Chem. A* **2005**, *109*, 5144−5152.
(75) Jezierska, A.; Panek, J.; Borstnik, U.; Mavri, J.; Janezic, D. *J. Phys. Chem. B* **2007**, *111*, 5243−5248.
(76) Klein, R.; Mennucci, B.; Tomasi, J. *J. Phys. Chem. A* **2004**, *108*, 5851−5863.
(77) Pennanen, T.; Lantto, P.; Sillanpaa, A.; Vaara, J. *J. Phys. Chem. A* **2007**, *111*, 182−192.
(78) Kirchner, B.; Hutter, J. *J. Chem. Phys.* **2004**, *121*, 5133−5142.
(79) Mcgrath, M. J.; Siepmann, J. I.; Kuo, I. F. W.; Mundy, C. J. *Mol. Phys.* **2007**, *105*, 1411−1417.
(80) Raugei, S.; Klein, M. L. *J. Phys. Chem. B* **2001**, *105*, 8212−8219.
(81) Kuo, I.-F.; Mundy, C.; Eggimann, B.; McGrath, M.; Siepmann, J.; Chen, B.; Vieceli, J.; Tobias, D. *J. Phys. Chem. B* **2006**, *110*, 3738−3746.
(82) Reed, A. E.; Weinstock, R. B.; Weinhold, F. *J. Chem. Phys.* **1985**, *83*, 735−746.
(83) Jensen, F. *Introduction to Computational Chemistry*; Wiley: Chichester, 2007.
(84) Klamt, A.; Schuurmann, G. *J. Chem. Soc., Perkin Trans.* **1993**, 799−805.
(85) Car, R.; Parrinello, M. *Phys. Rev. Lett.* **1985**, 55, 2471.
(86) "CPMD V3.8 Copyright IBM Corp 1990−2007, Copyright MPI für Festkörperforschung Stuttgart 1997−2001"; see also www.cmpd.org.
(87) Becke, A. D. *Phys. Rev. A* **1988**, *38*, 3098−3100.
(88) Perdew, J. P. *Phys. Rev. B* **1986**, *33*, 8822−8824.
(89) Troullier, N.; Martins, J. L. *Phys. Rev. B* **1991**, *43*, 1993−2006.
(90) Kleinman, L.; Bylander, D. M. *Phys. Rev. Lett.* **1982**, *48*, 1425−1428.
(91) Odelius, M.; Kirchner, B.; Hutter, J. *J. Phys. Chem. A* **2004**, *108*, 2044−2052.
(92) Nose, S. *J. Chem. Phys.* **1984**, *81*, 511−519.
(93) Hoover, W. G. *Phys. Rev. A* **1985**, *31*, 1695−1697.
(94) Martyna, G. J.; Klein, M. L.; Tuckerman, M. *J. Chem. Phys.* **1992**, *97*, 2635−2643.
(95) Wannier, G. H. *Phys. Rev.* **1937**, *52*, 191−197.
(96) Marzari, N.; Vanderbilt, D. *Phys. Rev. B* **1997**, *56*, 12847−12865.
(97) Ahlrichs, R.; Bar, M.; Haser, M.; Horn, H.; Kolmel, C. *Chem. Phys. Lett.* **1989**, *162*, 165−169.
(98) Eichkorn, K.; Treutler, O.; Ohm, H.; Haser, M.; Ahlrichs, R. *Chem. Phys. Lett.* **1995**, *242*, 652−660.
(99) Schafer, A.; Huber, C.; Ahlrichs, R. *J. Chem. Phys.* **1994**, *100*, 5829−5835.
(100) Huber, H.; Dyson, A. J.; Kirchner, B. *Chem. Soc. Rev.* **1999**, *28*, 121−133.
(101) Kirchner, B.; Hutter, J.; Kuo, I. F. W.; Mundy, C. J. *Int. J. Mod. Phys. B* **2004**, *18*, 1951−1962.
(102) Martyna, G. J.; Tuckerman, M. E. *J. Chem. Phys.* **1999**, *110*, 2810−2821.